

Optimization of Iris Codes for Improved Recognition

Nitin K. Mahadeo, Andrew P. Papliński, Sid Ray
Clayton School of Information Technology
Monash University

{Nitin.Mahadeo, Andrew.Paplinski, Sid.Ray}@monash.edu

Abstract

The texture of the iris is commonly represented as an iris code in iris recognition systems. While several approaches have been presented for generating iris codes, relatively few comparison techniques have been proposed. In this paper, we take advantage of the availability of several frames from an iris video to create a single optimized iris code. This is achieved by performing both row-wise and column-wise optimization of iris codes. Inconsistent bits are accurately detected and masked in the final iris code. Our experiments demonstrate that by exploiting variations within the comparison scores of different rows and columns of N frames, we are able to derive the number of consistent bits in the final iris code thereby resulting in significant improvement in recognition performance. We compare our algorithm with well-known methods, namely, Fragile bit masking, Signal fusion and, two Score Fusion techniques. Experimental results on a dataset of 986 iris videos show that the proposed method is encouraging and comparable to the best algorithms in the current literature. To our knowledge, this is the first work that makes use of the best rows and columns from different frames in an iris video to improve performance.

1. Introduction

Several biometric systems have been developed by governments and businesses with the aim of identifying individuals in a more secure and reliable manner. As a result of the high complexity of the iris texture, it can be used for identification and verification. The iris code is obtained by applying a texture filter on the iris region to extract a binary representation of the iris pattern. Numerous coding techniques have been developed over the years for iris recognition. However, two-dimensional Gabor filtering proposed by Daugman in 1993 remains the traditional approach [2].

Fractional Hamming Distance (HD) is used to evaluate the disparity between two iris codes during the comparison or matching stage. This involves two Boolean operators, the Exclusive-OR operator (XOR) and the AND oper-

ator. The XOR operator, \otimes , identifies differences between complimentary pairs of bits between two iris codes and an AND operator, \cap , ascertains that bits being compared exclude noise arising from eyelids, eyelashes and reflections. This is shown in expression (1)

$$HD = \frac{\sum_{i=1}^n (A_i \otimes B_i) \cap (A_i^m \cap B_i^m)}{\sum_{i=1}^n (A_i^m \cap B_i^m)} \quad (1)$$

where n is the total number of bits in an iris code, A_i and B_i are the bits for a given pair of iris codes and their corresponding bit masks A_i^m and B_i^m .

A suitable decision threshold is applied for the desired False Accept Rate (FAR) or False Reject Rate (FRR) according to the environments and requirements. It is certainly desirable in biometric systems to keep the error rates as low as possible. To this end, one of the avenues investigated by researchers concentrates mainly on enhancing the quality of segmented iris patterns which in turn translates into improved recognition performance. In [20], adaptive histogram equalization is applied on isolated iris patterns to improve its contrast prior to encoding. Vatsa *et al.* [21] apply different image enhancement techniques on the segmented iris. A high quality iris image is subsequently obtained by adopting a support vector machine based learning approach. Multiple frames from an iris video are averaged into a single frame using signal fusion to improve performance in [7][8]. In their experiments, Hollingsworth *et al.* use varying number of frames and masking. The optimal parameters are determined for optimal performance. In [17], local histogram equalization is applied on the iris image followed by phase-based matching. The second avenue adopted by researchers focuses primarily on different feature extraction techniques with the aim of capturing the most discriminating features in the iris. These include Haar wavelets, independent component analysis and directional filter banks [11]. A thorough evaluation and implementation of different coding techniques used in iris recognition systems can be found in [9].

Nonetheless, little consideration has been given to iris code comparison techniques. The existence of “fragile” bits

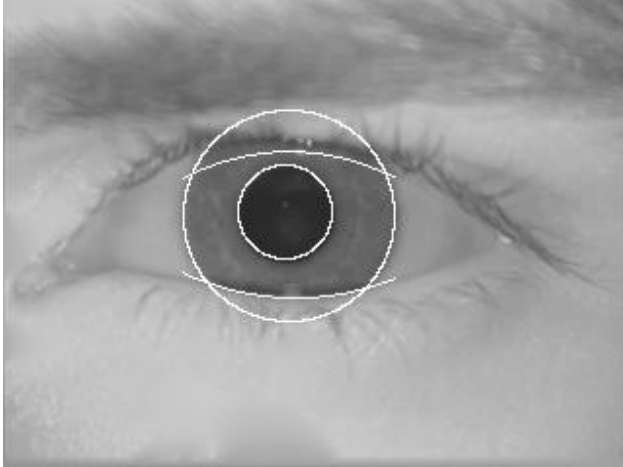


Figure 1. Example of a segmented iris region in a frame

was first suggested by Bolle *et al.* in [1]. This was further investigated by Hollingsworth *et al.* in [6]. It involves bits which are equally likely to flip to zero or one in different iris codes of the same eye as they lie close to the imaginary and real axes. Screening of these fragile bits in the comparison stage has shown to deliver superior performance. In [3], an iris matching method based on a weight map learned by training iris images of the same class is proposed by the authors. The weight map is updated during the iris recognition process and its robustness is improved by appointing the correct weights to feature codes. A bit reliability-driven matching approach is implemented by Rathgeb and Uhl in [19]. Information on consistent bits are updated, refined and stored after successful authentications to improve accuracy. Dozier *et al.* investigate the number of bits needed for iris recognition in [4]. Bit inconsistency and genetic search are used to reduce the number of iris bits without affecting performance. In [13], Ma *et al.* compute the average Hamming distances by comparing N iris codes. Krichen *et al.* adopt the same approach but instead use the minimum Hamming distance comparisons of N iris codes [12]. Both the minimum and average score fusion methods would require N iris codes of each individual to be stored in the database for matching.

The contribution of this study is the proposal of an optimized iris code with high number of consistent bits and low number of fragile (inconsistent) bits. This is achieved by performing both row-wise and column-wise optimization of iris codes from N iris frames. The number of inconsistent bits in each iris code is computed and masked. This work demonstrates that rather than looking at the iris code only as whole entity, the best rows and columns originating from different iris codes can be combined together to form an enhanced version. This paper is organized as follows. In Section 2, the amount of consistent and inconsistent bits

across different frames from the same iris video is investigated. The procedure for developing the optimized iris code is presented in Section 3. Section 4 discusses the proposed algorithm followed by its evaluation in Section 5. Finally, our discussions and conclusions are presented in Section 6 and Section 7.

2. Consistent vs. Inconsistent bits

Typically, iris codes are compared to each other using fractional HD and a decision threshold is used to determine if the subject is genuine or an impostor. In order to highlight the properties of iris codes, the following experiment is conducted. For a given video, twenty-six frames of successfully segmented iris are selected, unwrapped and their respective iris codes are obtained by applying Log-Gabor filter on their iris patterns. An example of an iris region segmented using the method proposed in [15] is shown in Figure 1. The HD scores between each iris code and its remaining twenty-five counterparts are then computed as shown in expression (2). For example, the Hamming distances between the iris code I_1 and the remaining iris codes $I_2 \dots I_N$ are computed. The same operation is repeated on the remaining iris codes totalling $N \times (N - 1)$ computations.

$$\begin{aligned}
 I_1 &\rightarrow I_2, I_3, I_4, \dots, I_N \\
 I_2 &\rightarrow I_1, I_3, I_4, \dots, I_N \\
 &\vdots \\
 I_N &\rightarrow I_1, I_2, \dots, I_{N-1}
 \end{aligned} \tag{2}$$

Boxplots of the Hamming distances obtained from the comparisons of each iris code with the remaining twenty-five iris codes from the same gallery set are shown in Figure 2. It can be observed that variations from one iris code to another can be significant even though they come from the same gallery. For example, boxplot of iris code of frame 1 and frame 26 perform poorly compared to the other box-

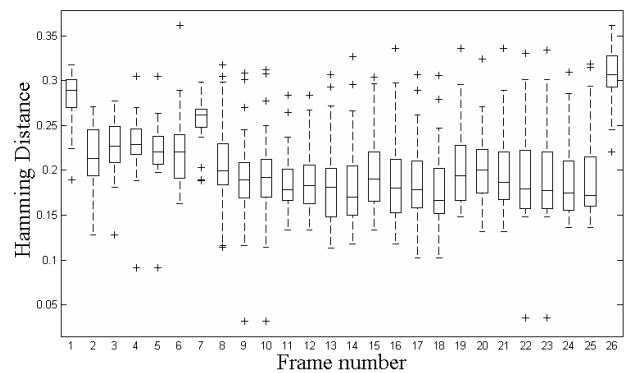


Figure 2. Boxplots comparing the Hamming Distance scores of twenty-six frames from the same gallery.

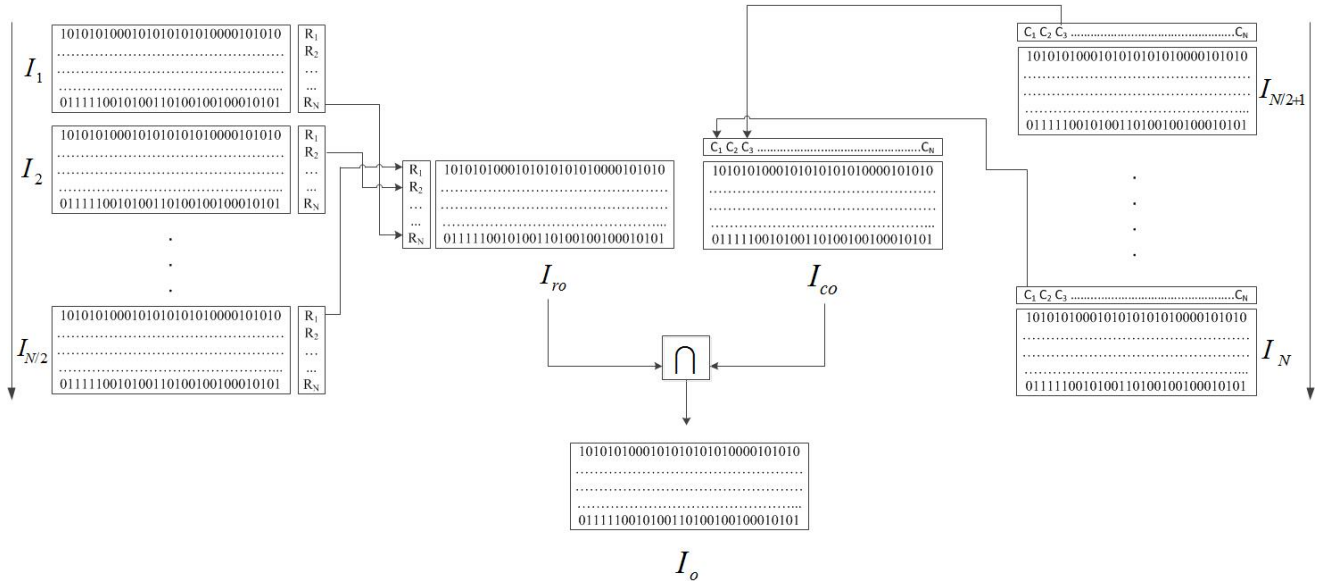


Figure 3. The proposed algorithm for selecting the best rows and columns from N iris codes. Iris codes I_1 to $I_{N/2}$ are used to obtain the row-optimized iris code I_{ro} and iris codes $I_{N/2+1}$ to I_N are used to construct the column-optimized iris code I_{co} . An AND \cap operation between I_{ro} and I_{co} yields the final iris code, I_o .

plots as suggested by their relatively high Hamming Distances. Boxplot of iris code of frame 18 achieves the lowest mean HD, 0.18, indicating that it has a higher number of consistent bits resulting in relatively low HD when compared to other iris codes from the same gallery. On the other hand, boxplot of iris code of frame 7 achieves the lowest standard deviation (σ), 0.028, while boxplot of iris code of frame 23 has the highest σ , 0.058. The above observations seems to suggest that there is significant variability from one iris code to another. This also implies that frames contain both consistent and inconsistent bits in varying proportions. Iris codes with higher degree of consistent bits and/or lower degree of inconsistent bits would perform better while iris codes with lower degree of consistent bits and/or higher degree of inconsistent bits would perform poorly.

As confirmed by Hollingsworth *et al.* in [6], the presence of fragile (inconsistent) bits in iris codes influence performance. However, this has been typically dealt with by considering the lower quartile of complex numbers resulting in the masking of real bits close to the imaginary axis and masking of imaginary bits close to the real axis. As demonstrated in our experiments, the number of fragile bits varies from one gallery set of images to another. One of the objectives of this work is to develop an optimal way of identifying the number of inconsistent bits in an iris code. A detailed approach for developing an optimized iris code is presented in the following section followed by experiments carried out in order to determine the optimal number of iris codes required.

3. Proposed Iris Code Optimization Method

The proposed technique consists of three main stages. In the first and second stages, row-wise and column-wise optimization are examined. In the third stage, we describe how bits found to be inconsistent are detected and masked in the final iris code.

3.1. Selecting The Best Rows

Based on our investigation in Section 2, we are aware that different iris codes contain varying amount of consistent and inconsistent bits. We therefore proceed by finding the best rows from all available iris codes i.e., rows with the highest number of consistent bits are chosen.

Consider N iris codes from a given gallery set of images where N is an even number. As shown in Figure 3, for row-wise optimization, iris codes, I_1 to $I_{N/2}$ are used. Iris codes $I_{N/2+1}$ to I_N are used for column-wise optimization. This approach is adopted in order to ensure that the most consistent bits across a wider range of frames are chosen. The HD score of each row of each iris code is computed with the corresponding rows in the remaining ones. In the following example, we discuss how the first row, R_1 , is selected out of $N/2$ iris codes. The HD score of the first row, R_1 of iris code I_1 is computed with the remaining first rows of iris codes I_2 to $I_{N/2}$. Similarly, the HD score of the first row, R_1 of iris code I_2 is computed with the remaining first rows of iris codes I_1 to $I_{N/2}$, excluding I_2 this time. The same process is repeated for the remaining R_1 up to iris code $I_{N/2}$. This leaves us with $N/2 \times (N/2 - 1)$ HD score

comparisons for the first row R_1 out of $N/2$ iris codes. The mean Hamming distances, $\mu_1 \dots \mu_{N/2}$, for each row comparison is then computed. Finally, the row of the iris code with the lowest mean score is selected as shown in expression (3).

$$R_i = \min(\mu_1, \dots, \mu_{N/2}) \quad (3)$$

This process is repeated for the remaining rows, $R_2 \dots R_N$ and the optimal rows are selected in a similar manner. Figure 3 is an illustration of the above procedure where the optimal rows are selected from iris codes I_1 to $I_{N/2}$. In the given example, the first row R_1 is selected from iris code $I_{N/2}$ while the last row, R_N is taken from iris code I_1 . The final iris code is referred to as the row-wise optimized iris code, I_{ro} . One way of looking at the above algorithm is that it identifies which row performs best and this is subsequently used to build I_{ro} . The index of the best row of a given template is stored and the row-optimized iris code can be built based using the corresponding rows with the lowest mean Hamming distances. The same rows are in turn selected for the iris mask, M_{ro} . Figure 4 shows an example of the reconstructed iris pattern and its respective mask built from the optimal rows of iris patterns obtained from the row-wise optimization process.

3.2. Selecting the Best Columns

Here, the same procedure is implemented using a column-wise approach instead of row-wise. The best columns out of iris codes $I_{N/2+1}$ to I_N are chosen and the column optimized iris code, I_{co} and iris mask M_{co} are constructed. As shown in our example in Figure 3, here column C_3 from iris code $I_{N/2+1}$ is selected and column C_1 from iris code I_N to build the column-wise optimized iris code, I_{co} . The same columns are selected for the iris mask, M_{co} . It should be noted that a different set of iris codes are chosen to build I_{co} . For example, if four iris codes are selected, the first two individual iris codes, I_1 and I_2 are used to build I_{ro} and the remaining two iris codes, I_3 and I_4 iris codes are used to construct I_{co} . Ideally, the difference between the row-optimized iris code I_{ro} and the col-optimized iris code I_{co} should be very small. However, as shown in our experiments, this is not always the case.

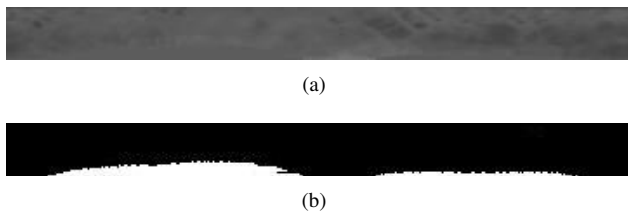


Figure 4. An example of the (a) iris pattern and the (b) iris mask reconstructed using the best rows identified by the row-wise selection technique.

3.3. The Optimal Iris Code and Iris Mask

In the final part of the proposed approach, our aim is to build an optimal iris code with the following properties. Firstly, only bits which are consistent in both iris codes, I_{ro} and I_{co} are considered. This would ascertain that the most consistent bits found in both the row-wise and column-wise operations are preserved. Secondly, bits which are not common to both I_{ro} and I_{co} are considered to be inconsistent and should not be used in our computations. Combined together, these two properties ensure that the final iris code has a maximum number of consistent bits and minimal number of inconsistent bits. This is achieved in the following manner. The optimal iris code, I_o , is obtained by performing an AND, \cap , operation between I_{ro} and I_{co} respectively as shown in expression (4). This ensures that only bits consistent in iris codes I_{ro} and I_{co} are retained.

$$I_o = I_{ro} \cap I_{co} \quad (4)$$

The second part involves the detection of “inconsistent” (disagreeing) bits. This is achieved using the XOR operator, \otimes which detects disagreeing bits between I_{ro} and I_{co} . This is shown in equation (5) and the result of this operation is stored in D .

$$D = I_{ro} \otimes I_{co} \quad (5)$$

Finally, the optimal iris mask, M_0 is built using the OR operator, \cup as defined in expression (6). The result of this operation ensures that the final mask accommodates for noise from disagreeing bits, D , the column-wise optimized mask, M_{co} and the row-wise optimized mask, M_{ro} .

$$M_o = M_{co} \cup M_{ro} \cup D \quad (6)$$

4. Experiments

The Multiple Biometric Grand Challenge (MBGC) version 2 dataset is used in our experiments. It consists of 986 Near Infrared iris video sequences acquired using an LG 2200 camera. The dataset consists of both right and left eyes. The number of videos per subject varies between one and seven and the time lapse between the video capture for each subject ranges between one and nine weeks [18]. We first start by considering only optimal frames in iris videos. This would ensure that an improvement is made as a result of the proposed algorithm and not as a consequence of frame quality. Several methods have been proposed in the literature on iris image quality assessment. We refer the reader to the following papers for more information on frame quality assessment methods developed for iris recognition systems [5][14][10]. In this work, iris videos are processed and high quality frames are obtained using the method described in [14]. The number of high quality frames obtained for each video will vary depending on its quality and length. The first video of each subject is

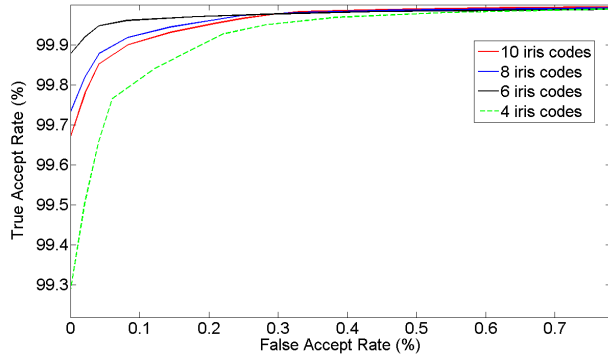


Figure 5. ROC curves for four, six, eight and ten iris codes.

No. of frames	FRR(%) @ FAR=0.001(%)	EER(%)
4	0.2795	0.1007
6	0.0358	0.0188
8	0.0691	0.0859
10	0.1128	0.1034

Table 1. The optimal iris codes built using six frames delivers better recognition performance than those derived from four, eight and ten frames.

considered to be the gallery set and the remaining videos are regarded as the probe set. All the extracted high quality iris frames are segmented and unwrapped onto a regular frame based on the rubber sheet model proposed by Daugman to compensate for varying sizes of captured iris frames [2][15]. The isolated iris patterns are encoded using Log-Gabor wavelets to obtain their respective iris codes [16].

In Section 4.1, the optimal number of frames required for building the optimized iris code I_o is determined and in Section 4.2 we demonstrate how the number of disagreeing bits can vary from one video to another. Section 5 compares the proposed approach with other methods.

4.1. Optimal Number of Frames

The number of iris codes required to form an optimal one is investigated in this section. Four high quality frames are initially selected and the optimized iris code is created as per the proposed approach described in Section 3. This experiment is then repeated using six, eight and ten frames respectively. Their ROC curves are shown in Figure 5. It can be observed that the 4-frame and the 10-frame plots perform poorly compared to the 6-frame and 8-frame curves. Overall, the curve where the optimal iris codes are derived from six individual iris codes performs significantly better than the rest.

This is confirmed by the results tabulated in Table 1 where EER is the Equal Error Rate, FAR is the False Accept Rate and FRR is the False Reject Rate. As the number of frames is increased from four to six, there is a sig-

nificant drop in the error rate, from 0.1007% to 0.0188%. It can also be observed that the 6-frame and the 8-frame curves have the lowest error rates. However, as the number of frames is increased from eight to ten, the error rate rises to 0.1034%. It should be mentioned that number of frames required to create the optimal iris code will vary depending on the dataset and frame quality. Based on the above figures, it can be deduced that the optimal number of iris codes required to build an optimized one for this dataset is six. This implies that the optimal equilibrium for retention of consistent bits and elimination of inconsistent bits in the optimized iris codes has been reached.

4.2. Performance Evaluation

The number of disagreeing (inconsistent) bits, D , between the row-optimized iris code I_{ro} and the column optimized iris code I_{co} is computed as per expression (5) in Section 3.3. This operation is carried out using four, six, eight and ten frames respectively. The boxplots in Figure 6 shows how the percentage of disagreeing bits varies with the number of frames used to build the optimized iris code, I_o . As per the figures in Table 2, there is an increase in the average number of disagreeing bits, μ , as the number of frames used is increased. On the other hand, a drop in the standard deviation, σ , is recorded as we move from four to ten iris codes. No clear trend is detected in the interquartile range. It is noteworthy to mention that the six-frames plot has the least number of outliers. Based on the above numbers, it is interesting to note that the effect of increasing the number of frames translates into better performance up to a certain limit as shown in our experiments.

This can be regarded as a dual optimization problem where the right balance of consistent and inconsistent bits needs to be reached for optimal performance. In this case, using four frames only to build the optimal iris code would mean that there is insufficient masking and detection of inconsistent bits. Seemingly, the right balance for the de-

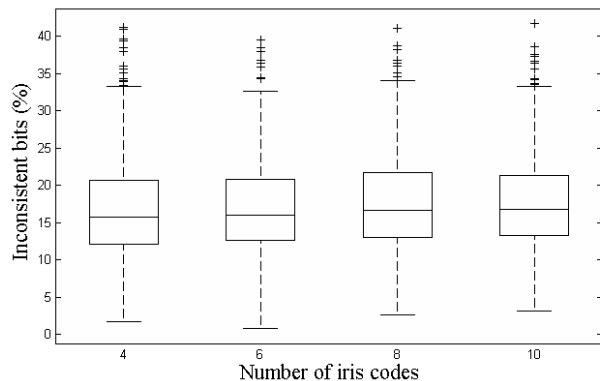


Figure 6. Boxplots of the percentage of disagreeing bits for four, six, eight and ten iris codes respectively.

D(%)	4 frames	6 frames	8 frames	10 frames
μ	16.88	17.11	17.63	17.84
σ	6.52	6.01	6.02	5.91
IQR	8.52	8.01	8.61	8.10

Table 2. Analysis in the variations of disagreeing bits, D, with number of frames used to compute the optimized iris codes.

tection of consistent and inconsistent bits occurs when six frames are used as indicated by its low EER. On the other hand, as shown in Table 2, the effect of increasing the number of frames leads to more masking. In the process, the probability of consistent bits being masked is also higher leading to a drop in performance when eight and ten iris codes are used to build the optimal one. Another effect of using an increasing number of iris codes to derive the optimal one is the introduction of more noise factors. In addition, different iris frames have different degree of occlusion, i.e., not all iris codes have the same amount of valid iris data. This could potentially lead to rows and columns with significant masking being chosen to build the optimal ones as they deliver better performance in row-wise and column-wise comparison. However, more masking means less valid bit comparisons thereby affecting the overall performance.

5. Comparison with previous methods

The performance of the proposed technique is compared with other methods in this section. The implementation details are also discussed.

5.1. 1-to-1 & N-to-1 Comparisons

The Signal Fusion method proposed by Hollingsworth *et al.* is implemented [7]. It consists of averaging of N frames to create a single average image. In the same manner as the work performed in [6, 8], fragile bit masking is implemented to screen complex coefficients which lie too close to the axes and might end up as a zero or a one in different iris codes of the same iris image. In our experiments, this is referred to as the 1-1 Signal Fusion-Fragile comparison. Another approach adopted by researchers is the enrolment of multiple frames. A single probe image is compared to N gallery images resulting in N Hamming distance scores. Ma *et al.* [13] take the average of the N Hamming distances to obtain a single score. This implementation is referred to as N-1 Score Fusion-Avg comparison. On the other hand, Krichen *et al.* [12] take the minimum of the N Hamming distance scores to obtain the final Hamming distance score. We term this as N-1 Score Fusion-Min comparison. In our proposed method, N frames are selected to build a single optimal iris code, I_o .

In line with previous matching schemes, we test the proposed algorithm in the following manner. N frames are

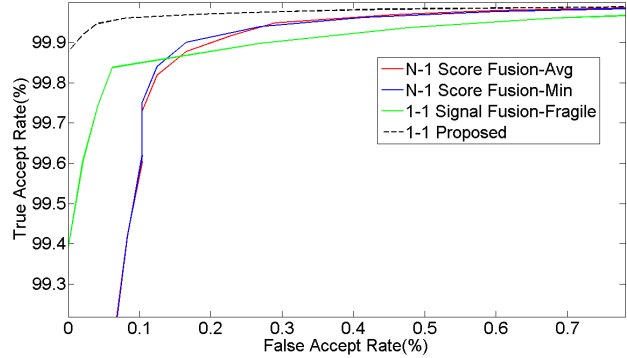


Figure 7. The proposed method performs better than Signal Fusion and Score Fusion methods

Method	OP(%)	d'	EER(%)
N-1 Score Fusion-Min	0.9060	6.093	0.1041
1-1 Signal Fusion-Fragile	0.1727	5.793	0.1032
N-1 Score Fusion-Avg	0.8168	6.049	0.1022
1-1 Proposed	0.0358	6.676	0.0188

Table 3. The performance of the proposed method compared to other implementations.

taken from the gallery set to create the optimized iris code. The same operation is performed on the probe sets to obtain their respective iris codes. For our experiments, $N = 6$ and the same dataset is used. The ROC curves of the different implementations discussed above are shown in Figure 7 and the results are tabulated in Table 3 where d' is the decidability index, OP is the operating point which gives us the FRR value at 0.001% FAR. Both the ROC curves of the Score Fusion-Min and Score Fusion-Average methods closely follow each other. However, they have relatively high operating points compared to the other methods implemented. On the other hand, the Signal Fusion-Fragile method achieves a comparably low operating point but takes a longer time to reach a high Accept Rate. The proposed method achieves the lowest operating point and reaches a high Accept Rate quicker than its counterparts. As indicated by its low EER, high d' and low OP, the proposed method performs significantly better than both Signal Fusion and Score Fusion methods.

6. Discussions

In the proposed approach, using four frames to build the optimal iris code would imply that there is still a high number of inconsistent bits in the final iris code as indicated by the comparably high EER. As we move from four to six iris codes, there is a significant drop in the EER. This is due to higher number of consistent bits and lower number of inconsistent bits resulting in more reliable HD scores. Beyond

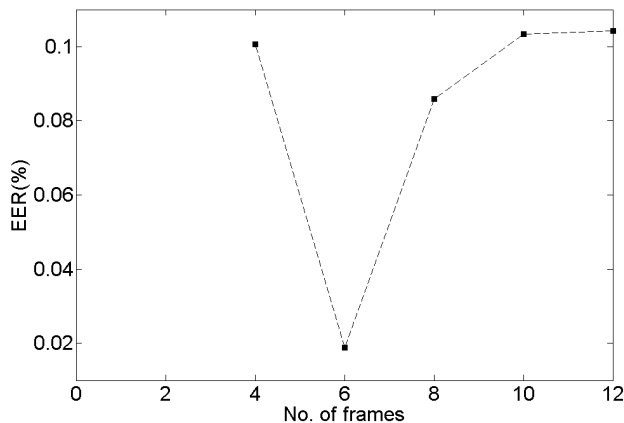


Figure 8. Change in EER with No. of frames used to build the optimal iris code.

this point, as shown in Figure 8, using eight, ten and twelve iris codes causes the EER to increase and performance is affected. As demonstrated in our experiments, more frames leads to more masking. The result is that there is less valid bit comparisons resulting in a rise in error rates.

In addition to performing comparably better than both N-1 Average and N-1 Minimum Score Fusion methods, the proposed algorithm takes only $1/N$ of the storage space. Identification of fragile bits for masking using a constant threshold such as the lower quartile rate does not always lead to optimal performance [22]. This could potentially lead to consistent bits being masked in the process or inconsistent bits being ignored. As shown in our experiments, the number of inconsistent bits can vary significantly from one iris code to another. In contrast, in this work, we are able to accurately determine the number of inconsistent bits present in each optimized iris code. By masking the appropriate number of inconsistent bits in each iris code valuable information is not lost and performance is improved.

In traditional iris recognition systems, in order to compensate for rotational inconsistencies, iris templates are shifted to the right and left and the lowest HD is chosen [2][16]. In our experiments, the same approach is adopted. When selecting the best rows, they are shifted eight bits to the left and to the right and the row with the smallest HD score is chosen. We also adopt the same approach when selecting the best columns. Only four shifts to the right and to the left are considered in this case since column length is significantly shorter than row length in a typical iris code.

7. Conclusion

In this work we have presented an accurate method for improving the performance in iris recognition systems. By efficiently selecting the best rows and columns in different

iris codes, consistent bits in the final iris code are preserved while inconsistent bits are eliminated in a reliable manner. Experimental results have demonstrated encouraging performance in terms of accuracy. In particular, a comparative study with other published methods is carried out. Both the performance evaluation and the comparison study validate our examination and understanding of iris codes. The proposed method could potentially be used in iris systems where low error rates are essential.

8. Acknowledgement

The authors would like to thank NIST and UND for granting access to the MBGC dataset.

References

- [1] R. Bolle, S. Pankanti, J. Connell, and N. Ratha. Iris individuality: a partial iris model. In *Pattern Recognition, 2004. ICPR 2004. Proceedings of the 17th International Conference on*, volume 2, pages 927–930 Vol.2, Aug 2004. 2
- [2] J. Daugman. How iris recognition works. In *Image Processing. 2002. Proceedings. 2002 International Conference on*, volume 1, pages I–33–I–36 vol.1, 2002. 1, 5, 7
- [3] W. Dong, Z. Sun, and T. Tan. Iris matching based on personalized weight map. *Pattern Analysis and Machine Intelligence, IEEE Transactions on*, 33(9):1744–1757, Sept 2011. 2
- [4] G. Dozier, K. Frederiksen, R. Meeks, M. Savvides, K. Bryant, D. Hopes, and T. Munemoto. Minimizing the number of bits needed for iris recognition via bit inconsistency and grit. In *Computational Intelligence in Biometrics: Theory, Algorithms, and Applications, 2009. CIB 2009. IEEE Workshop on*, pages 30–37, March 2009. 2
- [5] Y. Du, E. Arslanturk, Z. Zhou, and C. Belcher. Video-based noncooperative iris image segmentation. *Systems, Man, and Cybernetics, Part B: Cybernetics, IEEE Transactions on*, 41(1):64–74, Feb 2011. 4
- [6] K. Hollingsworth, K. Bowyer, and P. Flynn. The best bits in an iris code. *Pattern Analysis and Machine Intelligence, IEEE Transactions on*, 31(6):964–973, June 2009. 2, 3, 6
- [7] K. Hollingsworth, T. Peters, K. Bowyer, and P. Flynn. Iris recognition using signal-level fusion of frames from video. *Information Forensics and Security, IEEE Transactions on*, 4(4):837–848, Dec 2009. 1, 6
- [8] K. P. Hollingsworth, K. W. Bowyer, and P. J. Flynn. Image averaging for improved iris recognition. In *Proceedings of the Third International Conference on Advances in Biometrics, ICB '09*, pages 1112–1121, Berlin, Heidelberg, 2009. Springer-Verlag. 1, 6
- [9] A. K. Jain, P. Flynn, and A. A. Ross. *Handbook of Biometrics*. Springer-Verlag New York, Inc., Secaucus, NJ, USA, 2007. 1
- [10] N. Kalka, J. Zuo, N. Schmid, and B. Cukic. Estimating and fusing quality factors for iris biometric images. *Systems,*

- Man and Cybernetics, Part A: Systems and Humans, IEEE Transactions on*, 40(3):509–524, May 2010. 4
- [11] A.-K. Kong, D. Zhang, and M. Kamel. An analysis of iriscode. *Image Processing, IEEE Transactions on*, 19(2):522–532, Feb 2010. 1
- [12] E. Krichen, L. Allano, S. Garcia-Salicetti, and B. Dorizzi. Specific texture analysis for iris recognition. In T. Kanade, A. K. Jain, and N. K. Ratha, editors, *AVBPA*, volume 3546 of *Lecture Notes in Computer Science*, pages 23–30. Springer, 2005. 2, 6
- [13] L. Ma, T. Tan, Y. Wang, and D. Zhang. Efficient iris recognition by characterizing key local variations. *Image Processing, IEEE Transactions on*, 13(6):739–750, June 2004. 2, 6
- [14] N. Mahadeo, A. Paplinski, and S. Ray. Automated selection of optimal frames in nir iris videos. In *Digital Image Computing: Techniques and Applications (DICTA), 2013 International Conference on*, pages 1–8, Nov 2013. 4
- [15] N. Mahadeo, A. Paplinski, and S. Ray. Robust video based iris segmentation system in less constrained environments. In *Digital Image Computing: Techniques and Applications (DICTA), 2013 International Conference on*, pages 1–8, Nov 2013. 2, 5
- [16] L. Masek. Recognition of human iris patterns for biometric identification. Master’s thesis, University of Western Australia, 2003. 5, 7
- [17] K. Miyazawa, K. Ito, T. Aoki, K. Kobayashi, and H. Nakajima. A phase-based iris recognition algorithm. In *Proceedings of the 2006 International Conference on Advances in Biometrics, ICB’06*, pages 356–365, Berlin, Heidelberg, 2006. Springer-Verlag. 1
- [18] P. J. Phillips, P. J. Flynn, J. R. Beveridge, W. T. Scruggs, A. J. O’Toole, D. Bolme, K. W. Bowyer, B. A. Draper, G. H. Givens, Y. M. Lui, H. Sahibzada, J. A. Scallan, Iii, and S. Weimer. Overview of the multiple biometrics grand challenge. In *Proceedings of the Third International Conference on Advances in Biometrics, ICB ’09*, pages 705–714, Berlin, Heidelberg, 2009. Springer-Verlag. 4
- [19] C. Rathgeb and A. Uhl. Bit reliability-driven template matching in iris recognition. In *Image and Video Technology (PSIVT), 2010 Fourth Pacific-Rim Symposium on*, pages 70–75, Nov 2010. 2
- [20] A. Ross, R. Pasula, and L. Hornak. Exploring multispectral iris recognition beyond 900nm. In *Biometrics: Theory, Applications, and Systems, 2009. BTAS ’09. IEEE 3rd International Conference on*, pages 1–8, Sept 2009. 1
- [21] M. Vatsa, R. Singh, and A. Noore. Improving iris recognition performance using segmentation, quality enhancement, match score fusion, and indexing. *Systems, Man, and Cybernetics, Part B: Cybernetics, IEEE Transactions on*, 38(4):1021–1035, Aug 2008. 1
- [22] L. Yooyoung, R. J. Micheals, J. J. Filliben, and P. J. Phillips. Vasir: An open-source research platform for advanced iris recognition technologies. *Journal of Research of the National Institute of Standards & Technology*, 118, 2013. 7